International Geology Review

ISSN: 0020-6814 (Print) 1938-2839 (Online) Journal homepage: https://www.tandfonline.com/loi/tigr20

U-PB zircon tuff geochronology from the Karoo Basin, South Africa: implications of zircon recycling on stratigraphic age controls

Matthew P. McKay, Amy L. Weislogel, Andrea Fildani, Rufus L. Brunt, David M. Hodgson & Stephen S. Flint

To cite this article: Matthew P. McKay, Amy L. Weislogel, Andrea Fildani, Rufus L. Brunt, David M. Hodgson & Stephen S. Flint (2015) U-PB zircon tuff geochronology from the Karoo Basin, South Africa: implications of zircon recycling on stratigraphic age controls, International Geology Review, 57:4, 393-410, DOI: 10.1080/00206814.2015.1008592

To link to this article: https://doi.org/10.1080/00206814.2015.1008592

International Geology Review, 2015
Vol. 57, No. 4, 393–410, http://dx.doi.org/10.1080/00206814.2015.1008592

Taylor & Francis
Taylor & Francis Group

U-PB zircon tuff geochronology from the Karoo Basin, South Africa: implications of zircon recycling on stratigraphic age controls

Matthew P. McKay[a,b]*, Amy L. Weislogel[b], Andrea Fildani[c], Rufus L. Brunt[d], David M. Hodgson[e] and Stephen S. Flint[d]

[a]*Geological Survey of Alabama, Tuscaloosa, AL, USA;* [b]*Department of Geology and Geography, West Virginia University, Morgantown, WV, USA;* [c]*Statoil Research Center, Austin, TX, USA;* [d]*School of Earth, Atmospheric and Environmental Sciences, University of Manchester, Manchester, UK;* [e]*School of Earth and Environment, University of Leeds, Leeds, UK*

(*Received 26 November 2014; accepted 13 January 2015*)

Along the >650 km long southern margin of the Karoo Basin in South Africa, we traversed four evenly spaced stratigraphic transects and collected 22 samples of volcanic, air-fall tuffs thought to be distal deposits derived from the Permian–Triassic Southern Gondwanan volcanic arc. We present 469 new U-Pb zircon ages determined by sensitive high-resolution ion microprobe reverse geometry (SHRIMP-RG) at the Stanford–USGS Microanalytical Center in order to constrain the maximum depositional ages for the southern Karoo Basin strata. Weighted means of these youngest coherent zircon populations were selected to maximize the number of analyses while minimizing the mean square weighted deviation (MSWD) to increase the robustness and decrease the influence of Pb-loss and inheritance in determining the maximum depositional age. Maximum depositional ages for the marine Ecca Group range from 250 to 274 Ma, whereas in the conformably overlying terrestrial Beaufort Group maximum depositional ages ranged from 257 to 452 Ma. Across the southern Karoo Basin, the Ecca Group tuffs produce maximum depositional ages that young upward; however, the Beaufort Group tuffs yield maximum depositional ages that are geochronologically out of sequence. Furthermore, maximum depositional ages of the Beaufort Group tuffs are consistently older than ash ages within the underlying marine strata. Our results are supported by previously published U-Pb tuff zircon geochronology in the Karoo Basin and demonstrate that the presence of out-of-sequence, older tuff ages are repeatable in Beaufort Group tuffs along the southern margin of the basin. We propose that tuffs in the Karoo Basin are correlative with tuffs in southern South America, and that the age spectra of these tuffs were influenced by magmatic crustal recycling. We use these data to highlight the complexity of U-Pb zircon datasets from tuffs, address the use of U-Pb zircon ages to provide absolute age controls, and discuss the implications of these new age controls on the Permian-Triassic Karoo strata.

Keywords: geochronology; zircon; volcanic tuff; Karoo basin; Gondwanan volcanism

Introduction

The depositional age of clastic sedimentary strata is inherently difficult to date directly, since radiometric ages for clastic detritus reflect the age of the sediment source and not the depositional age of the sediment. Biostratigraphic ages can often be used to obtain relative geologic ages by correlating strata of interest to a Global Stratotype Section and Point (GSSP). GSSPs are defined by fossil assemblage, which precludes the direct correlation of sections between marine and terrestrial sediments. Biostratigraphic correlations, therefore, typically rely on lithostratigraphic classification, although sedimentary deposits are commonly time transgressive. Recent advances in sedimentary geochronology have demonstrated the tenuous nature of biostratigraphy-based ages and have shown that correlating strata to global events is tenuous without absolute age controls (Surpless *et al.* 2006). One approach for resolving the maximum depositional age of sedimentary strata is through radiometric dating of syneruptive minerals found in volcanic tuffs preserved as interbeds in sedimentary basin fill strata. Zircon U-Pb geochronology is the most frequently employed tool for estimating the eruptive age of a volcanic ash, which is a proxy for the depositional age of the encasing strata (Bowring and Schmitz 2003). This method requires the assumption that zircon within the ash is co-eruptive, and does not contain (1) older, inherited magmatic grains; (2) detrital zircon from sedimentary reworking and contamination of the ash; and (3) damaged grains that have undergone alteration and Pb-loss. U-Pb zircon data from tuffs do not always demonstrate a well-defined, single population. This suggests that tuffs might contain multi-age zircon populations. Therefore, the traditional assumption that zircon grains within tuffs are dominantly co-eruptive is at times flawed. Within the Karoo Supergroup of South Africa, multiple U-Pb

*Corresponding author. Email: mmckay@ogb.state.al.us

zircon studies have resolved complex spectra of ages (Coney *et al.* 2007; Fildani *et al.* 2007, 2009; Lanci *et al.* 2013; Rubidge *et al.* 2013), leading to conflicting age interpretations for the absolute, maximum depositional age of the strata. This problem makes the Karoo strata ideal to test commonly held assumptions that zircon within volcanic tuffs is dominantly co-eruptive and that these ages represent the depositional age of sedimentary strata.

The Karoo Supergroup is in part composed of the marine Ecca Group and the conformably overlying, terrestrial Beaufort Group (Veevers *et al.* 1994a). The Upper Beaufort Group has long been thought to contain the Permian–Triassic boundary, which was interpreted from biostratigraphic correlations (Smith and Ward 2001). A paucity of fossils, however, limits biostratigraphic controls within the Permian-to-Triassic Ecca and Beaufort Groups (Smith 1995). To circumvent limited biostratigraphic age controls with large uncertainties for the depositional age of the Karoo strata, recent studies have attempted to constrain the absolute age of the vertebrate fossil-defined Permian–Triassic boundary within the Karoo Supergroup strata using U-Pb geochronology on zircon from interbedded volcanic tuffs (Coney *et al.* 2007; Fildani *et al.* 2007, 2009), similar to the approach used to define the age of the GSSP Permian–Triassic boundary from tuffs within fossiliferous marine strata in southern China (252.28 ± 0.08 Ma; Shen *et al.* 2011). Fourteen volcanic-ash zircon U-Pb ages from the Beaufort Group in the central and southwestern Karoo Basin have yielded wholly Permian maximum depositional ages ranging from 266 to 252 Ma (Coney *et al.* 2007; Rubidge *et al.* 2013; Lanci *et al.* 2013). Zircons from 16 tuff samples from the underlying Ecca Group exposed in the southwestern Karoo Basin contain 12 Triassic and 193 Permian grains and yield maximum depositional ages ranging from 275 to 250 Ma (Fildani *et al.* 2007, 2009). The presence of the latest Permian zircon is also documented in detrital zircon ages from sandstones in the Ecca Group from the southwestern Karoo Basin (Vorster 2013). Thus, in spite of the geographically and stratigraphically restricted nature of existing tuff zircon U-Pb ages, it appears that the radiometric ages from interbedded tuffs in the Upper Ecca Group are younger than tuffs in the overlying Beaufort Group, which is not consistent with the upsection younging trend expected for ash deposits.

To address this apparent contradiction of older U-Pb zircon ages in the overlying Beaufort compared to younger ages in the underlying Ecca, we performed a regional study to sample tuffs from both the Ecca and Beaufort Groups across the southern Karoo Basin (Figure 1). We present 469 new U-Pb zircon single-grain ages to determine maximum depositional ages for 22 air-fall tuffs. Our results include the first age controls for deposition of the Ecca Group in the eastern Karoo Basin along with age controls throughout the entire Ecca Group and Lower Beaufort Group for four stratigraphic sections spaced across the southern Karoo Basin margin. These results demonstrate that tuffs from the Beaufort Group consistently yield zircon with U-Pb ages that overlap or are older than zircon from the tuffs in the underlying Ecca Group. Maximum depositional ages for the Ecca Group range from 274 to 249 Ma and are coeval across the southern margin of the basin. The maximum depositional ages from the overlying Beaufort Group however range from 274 to 255 Ma. In each of the four stratigraphic sections, the youngest maximum depositional age of the Beaufort Group tuffs is consistently older than the youngest maximum depositional age of the underlying Ecca

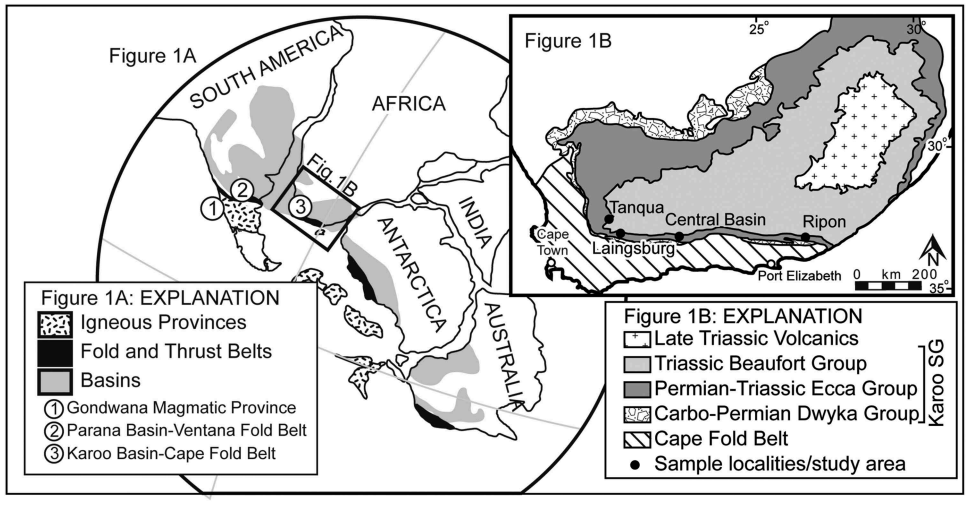

Figure 1. (A) Geology of Southern Gondwana (modified after Zeigler *et al.* 1983; Lawver *et al.* 1992; López-Gamundi and Rossello, 1998; Fildani *et al.* 2007) showing the relative locations of the Gondwanide Magmatic Province, Fold Thrust Belt, and Foreland Basin (i.e. Karoo Basin). (B) Geologic map of the Karoo Basin, South Africa (adapted from Catuneanu *et al.* 2002). Sample localities shown: Tanqua, Laingsburg, Central Basin, and Ripon depocentres.

Group. This relationship could be satisfied by three interpretations: (1) Ecca Group strata that crop out along the southernmost Karoo Basin are younger than the Beaufort Group strata exposed to the north, which would require a fundamental revision of the regional stratigraphic and/or structural framework; (2) the volcanic tuffs in the Beaufort Group do not contain syneruptive zircon that reflects the true depositional age; or (3) cryptic Pb-loss has selectively affected zircon in tuffs in the uppermost Ecca Group across the 650 km long southern margin of the basin, while not affecting zircon in Lower Ecca or overlying Beaufort Groups. We consider these competing hypotheses and examine the implications to explore the Permian–Triassic evolution of southern Gondwana.

Geologic background

The Ecca and Beaufort Groups of the late Carboniferous-Jurassic Karoo Supergroup accumulated as a flysch-to-molasse style succession within the Karoo Basin, a tectonically subsiding basin developed in the Gondwanan cratonic interior (Catuneanu *et al.* 2002; Tankard *et al.* 2009; Holt *et al.* 2015). The northeast–southwest elongate basin is bounded by the Cape Fold Belt to the west and south (Figure 1) that contains three clastic depositional areas: the Tanqua, Laingsburg, and Ripon depocentres. The Karoo Supergroup includes the basal fluvioglacial Dwyka Group (Crowell 1978), the overlying Ecca Group, and the Beaufort Group. Following deposition of the Dwyka Group, deep-water basinal environments shoaled upward into shallow-water, marginal marine environments during deposition of the Ecca Group. The lowermost Ecca Group is mudstone-dominated at the base (Prince Albert, Whitehill, Collingham, Vischkuil, and Tierberg formations) and is overlain by basin-floor, sandy turbidite strata (Skoorsteenberg, Laingsburg, and Ripon formations; Bouma and Wickens 1994; Catuneanu *et al.* 2002). The upper Ecca Group consists of submarine slope channel/levee systems (Fort Brown Formation; Hodgson *et al.* 2011) and shelf-edge and shelf clastics (Kookfontein and Waterford formations; Wild *et al.* 2009; Flint *et al.* 2011; Jones *et al.* 2013) that record diachronous filling of the basin (Rubidge 2000). The Beaufort Group records the transition to terrestrial deposystems and evolution of terrestrial vertebrates and macroflora (Groenewald and Kitching 1995; Smith 1995; Gastaldo *et al.* 2005). Interbedded throughout the Ecca and Beaufort strata are numerous air-fall volcanic tuffs thought to have been produced by a late Palaeozoic Gondwanan magmatic arc, the remnants of which are locally preserved as the Choiyoi and Puesto Viejo magmatic suites in South America (Veevers *et al.* 1994a; López-Gamundí 2006; Kleiman and Japas 2009; Rocha-Campos *et al.* 2011; López-Gamundí *et al.* 2013). Choiyoi and Puesto Viejo magmatism dates from ~276 to ~234 Ma and is responsible for air-fall ash deposits in the Paraná (Rocha-Campos *et al.* 2011) and Cuyo basins (Spalletti *et al.* 2008) in South America, in addition to the Karoo Basin in South Africa (Figure 1B), based on palaeogeography and geochemistry (López-Gamundi *et al.* 2006). The Choiyoi and Puesto Viejo magmatic suites, which are separated by a ~251–240 Ma tuff gap (Veevers *et al.* 1994b; Veevers 2004; Spalletti *et al.* 2008; Kleiman and Japas 2009), contain distinct zircon populations. The Permian Choiyoi Group contains an abundant Permian zircon population (Domeier *et al.* 2011; Rocha-Campos *et al.* 2011) with some mixing of mid-Permian (>260 Ma) and late Permian (250–260 Ma) zircon in late Permian tuffs (Rocha-Campos *et al.* 2006). The Triassic Puesto Viejo Group is dominated by recycled Permian (>260 Ma) zircon with few co-eruptive zircons (Spalletti *et al.* 2008; Domeier *et al.* 2011), interpreted to be due to assimilation of Permian country rocks during Triassic magmatic assent (Domeier *et al.* 2011). Weighted mean U-Pb ages for the Puesto Viejo Group range from ~260 Ma to ~230 Ma (Spalletti *et al.* 2008; Domeier *et al.* 2011; Ottone *et al.* 2014), even though it is generally accepted that Puesto Viejo magmatism occurred between 241 and 230 Ma (Kleiman and Japas 2009; Domeier *et al.* 2011).

U-PB methods and analyses

Twenty-two tuffs were sampled from four transects through formations of the Ecca and Beaufort Groups exposed along the southern Karoo Basin (Figure 1). Five samples were collected from the Tanqua depocentre in the western Karoo Basin and were integrated with previously published results from Fildani *et al.* (2007, 2009) and Lanci *et al.* (2013). Four new samples were collected from the southwestern Laingsburg depocentre to augment previously published data in the Laingsburg area (Fildani *et al.* 2007, 2009). In the eastern Ripon depocentre, 10 samples were collected along a single, continuous north-dipping transect. Three samples were collected from the Ecca Group in a mudstone-dominated, condensed section in the central Karoo Basin between the Laingsburg and Ripon depocentres (~22.5°E; Figure 1). Zircon grains were separated from samples using mineral separation techniques, including the use of a Franz magnetic separator to remove high U zircon that may yield discordant results (Sircombe and Stern 2002). Samples yielded between 0 and >200 zircon. Size, morphology, and inclusion density were not considered when selecting zircon for analysis in an effort to characterize the entire zircon population of an ash and not bias results toward prismatic, acicular, euhedral zircon populations. Catholuminescence images (Figure 2A) were used to target intermediate U (100–1000 ppm) and oscillatory zoned grain rims and avoid complex cores, when present. Sensitive high-resolution ion microprobe reverse geometry (SHRIMP-RG) analyses of zircon grains were conducted at the Stanford Microscopic Analytical Center under analytical conditions

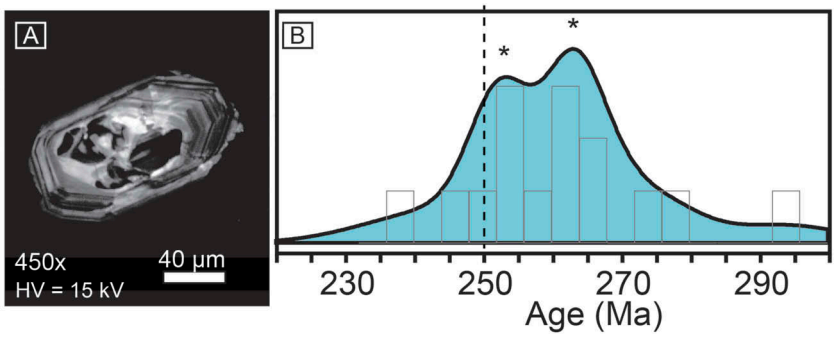

Figure 2. (A) Catholuminescence image of a zircon grain from a tuff in the Ecca Group showing zircon rim and core growths. (B) Kernel density estimate of sample 12ZA07. Populations between 230 and 300 Ma are identified with an asterisk.

similar to those of Barth and Wooden (2006). SHRIMP-RG results were calculated with reference to the R33 zircon standard (Black *et al.* 2004) and results were reduced using the SQUID2 software (Ludwig 2009).

Ages reported are from common-Pb corrected $^{206}Pb/^{238}$ U ratios. Of the 469 total single-grain analyses, 353 were accepted on the basis of low common-Pb concentrations, low uncertainty (<3%), and concordance. Grains were determined to be concordant if $^{238}U/^{206}Pb$ and $^{207}Pb/^{206}Pb$ ages overlapped within uncertainty. Anomalously old zircon grains (>300 Ma) were interpreted as inherited, xenocrystic, or detrital grains, while anomalously young, high-U or high common-Pb (≪~250 Ma) are dismissed as having been affected by Pb-loss or common-Pb contamination. Kernel density estimate (KDE) plots (Figure 2B) were used to interpret recycled, inherited zircon from likely autocrystic/co-eruptive zircon populations. Zircon age populations were identified to determine tuff maximum depositional ages, which if zircon grains are syneruptive autocrysts should equal the eruption age of the tuff. Population ages were then calculated from the weighted average of a coherent zircon population ($n \geq 3$) using Isoplot 3.75 (Ludwig 2008). Although calculating maximum depositional ages from coherent age populations commonly produces higher uncertainty compared with using the youngest single-grain age from a sample, it is viewed as a more robust age given the greater reproducibility. A table of analytical results and concordia diagrams are provided in Appendix B (see http://dx.doi.org/10.1080/00206814.2015.1008592). Maximum depositional age interpretations are reported in their sampled stratigraphic locations with numerical age interpretations (Figure 3) and schematically with associated errors (Figure 4) to demonstrate stratigraphic trends in tuff ages.

U-PB results and interpretation

Analysis of 22 ash samples from the marine Ecca and terrestrial Beaufort groups of the lower Karoo Supergroup yielded 116 pre-Permian, 223 Permian, and 14 Triassic concordant zircon ages of 469 total analyses. In many samples, zircon produced a dispersed range of ages (>20 Ma). While this age range could be due to mixing of different age domains within individual zircon grains during analysis, analytical uncertainty, or Pb-loss (Castiñeiras *et al.* 2010), magma system evolution is complex and commonly recycles older zircon into later eruption/emplacement events and some individual plutons have been resolved to be emplaced over a period of >10 Ma (Coleman *et al.* 2004; Miller *et al.* 2007; Schwartz *et al.* 2014). The suspected volcanic sources, the Choiyoi and Puesto Viejo igneous suites, are known to have large populations of recycled zircon (Spalletti *et al.* 2008; Domeier *et al.* 2011; Ottone *et al.* 2014). We therefore interpret this range to represent mixing of the zircon age population based on (1) high MSWD (1.6–17) of the weighted mean for Permian/Permo-Triassic zircon populations (Miller *et al.* 2007; Compston and Gallagher 2012); (2) lack of inherited cores interpreted from catholuminescence images; (3) the reproducibility of ages between several grains ($s \geq 3$); (4) concordance of the analyses; and (5) known history of the volcanic system. In order to avoid introducing bias toward inherited/recycled zircon age populations, maximum depositional ages are calculated from the weighted mean of the youngest, concordant zircon population (P_1) of three or more analyses as identified by kernel density plots to minimize the risk of producing an age affected by Pb-loss (Dickinson and Gehrels 2008) (Appendix B). Inherited zircon population ages (P_2) were interpreted using the same approach as on older, concordant zircon populations. This approach decreases the total number of analyses, which could negatively affect the uncertainty in the weighted mean age. The result, however, more likely represents the eruption age of the ash and in most cases produces higher precision ages and a lower MSWD. This approach differs from the method used by Lanci *et al.* (2013), where interpreted ash ages were calculated from all zircons between 300 Ma and 250 Ma and included all ages within a dispersed range of up to 20 million years. Results from previous geochronology studies on tuffs within the Karoo Supergroup (Coney *et al.* 2007; Fildani *et al.* 2007,

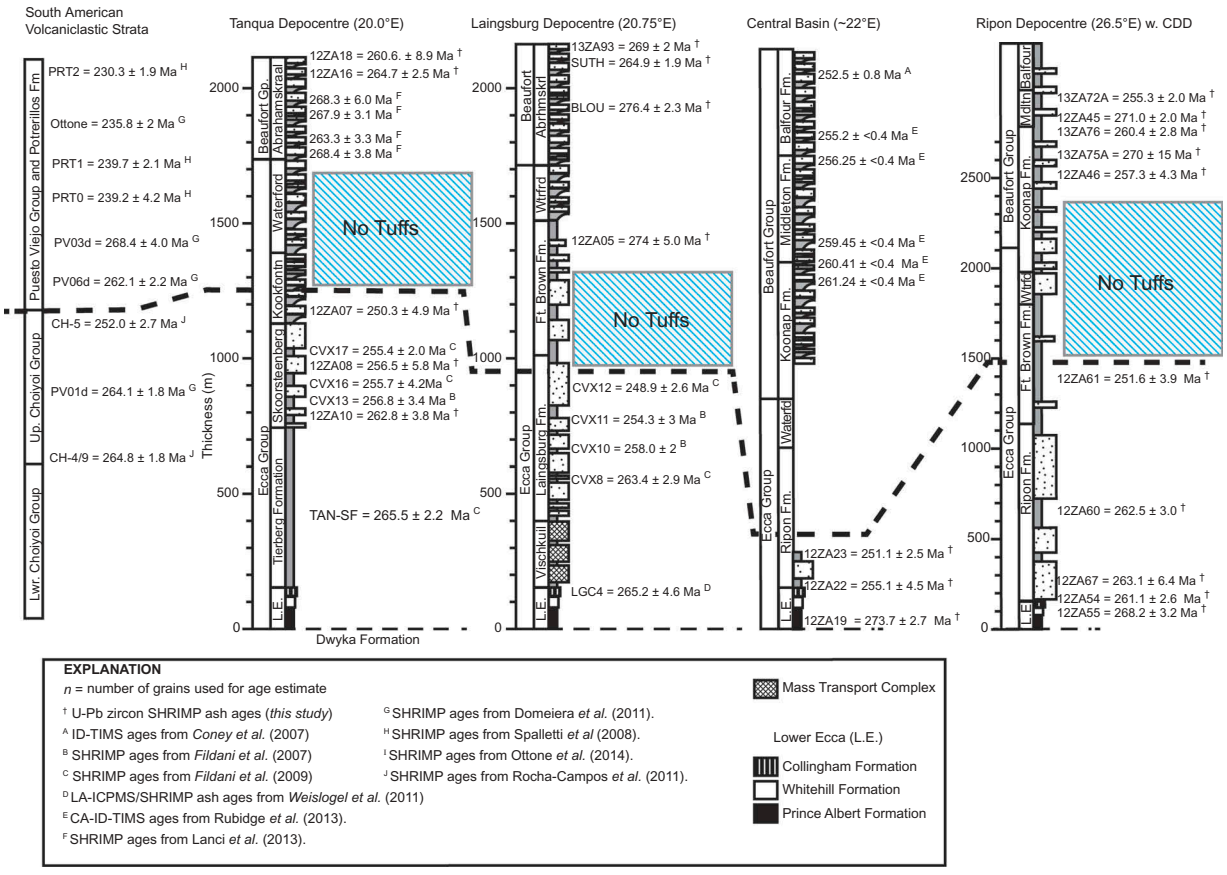

Figure 3. Chronostratigraphic correlation between the Karoo Supergroup and South American volcaniclastic strata (Puesto Viejo volcanics or equivalents). Karoo Supergroup ages are from Coney *et al.* (2007), Fildani *et al.* (2007, 2009), Weislogel *et al.* (2011), Lanci *et al.* (2013), Rubidge *et al.* (2013), and this study. South American volcanic ages are from Domeier *et al.* (2011), Spalletti *et al.* (2008), Rocha-Campos *et al.* (2011), and Ottone *et al.* (2014). Maximum depositional ages from this study are reported with the associated 95% confidence uncertainties at the sampled stratigraphic interval. The interval where tuffs were not present is identified by a striped pattern where observed in the Tanqua, Laingsburg, and Ripon depocentres. Sample locations are reported in Appendix A (see http://dx.doi.org/10.1080/00206814.2015.1008592). The individual analyses can be found in Appendix B. Karoo and South American Volcanics both show trends upsection where latest Permian volcanics yield ages that are younger than the overlying volcanic deposits.

2009; Lanci *et al.* 2013; Rubidge *et al.* 2013), tuffs within correlative basins (Rocha-Campos *et al.* 2006, 2011; Spalletti *et al.* 2008; López-Gamundi *et al.* 2013; Domeier *et al.* 2011), and Permo-Triassic crustal plutonic rocks (Pankhurst *et al.* 2014) in South America contained populations of inherited grains. Based on this known inheritance, indiscriminately including these older zircons in weighted age calculations is not a favourable approach to obtain reasonable maximum depositional ages for the Karoo tuffs. Therefore, our ages are presented as weighted averages of the youngest zircon population to avoid introducing statistical bias toward dominant inherited populations when determining tuff ages. These results are shown in stratigraphic order, with uncertainties reported at a 95% confidence level (Figure 3). Also provided are previously reported ages for the Karoo strata and reported ages of comparable South American volcanic suites.

Tanqua depocentre

Ecca Group

Three tuffs were sampled from the Ecca Group to augment the existing five tuff ages from Fildani *et al.* (2007, 2009) (location on Figure 1B). Results from samples collected from the Tanqua depocentre are described in ascending stratigraphic order. While tuffs are common throughout the section and the samples presented here represent only a small fraction of the tuffs in the Karoo strata, no volcanic deposits were found in the interval between sample 12ZA07 in the Ecca Group and 12ZA16 in the Beaufort Group.

Sample 12ZA10

The lowermost sample in the Tanqua depocentre is 12ZA10, which was collected from an ~3 cm-thick, green,

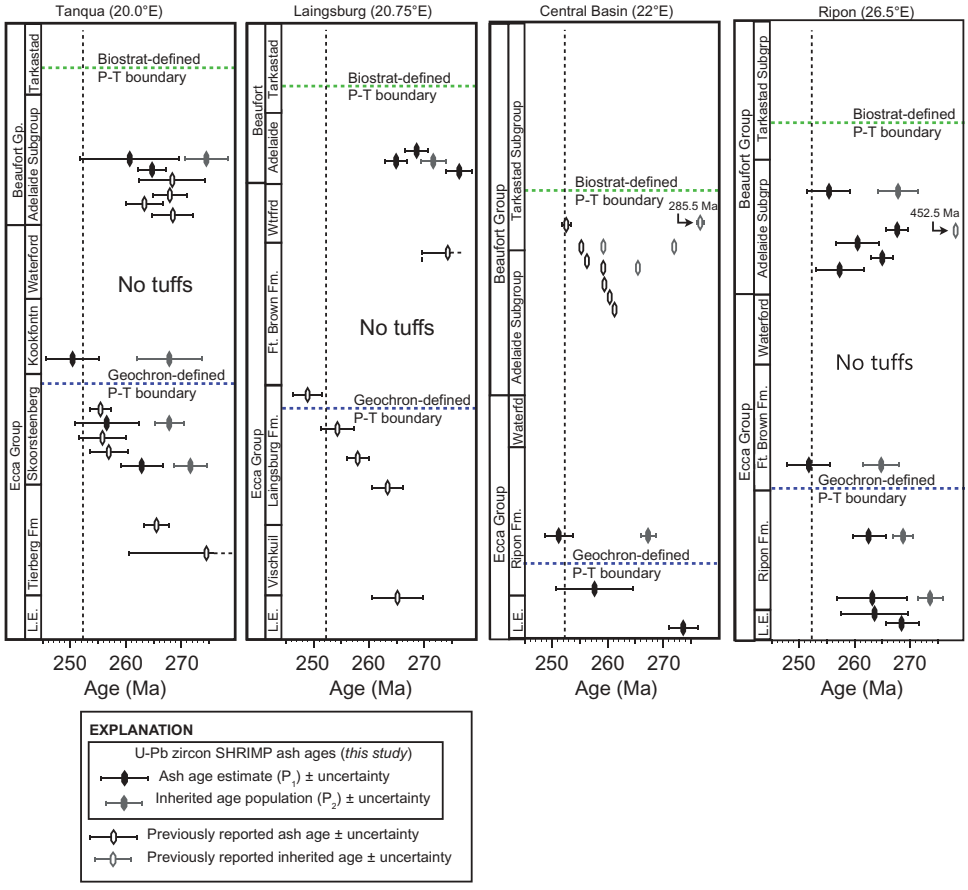

Figure 4. Maximum deposition ages, based on U-Pb zircon, from Figure 3, shown schematically, with associated error. In all four studied sections, maximum depositional ages young upsection in the lower and middle Ecca. Proceeding upsection, an interval is encountered with few to no tuffs. Above this tuff-free interval, U-Pb zircon-based maximum depositional ages are chaotic and older than in the underlying strata.

clay-textured tuff interbedded with mudstones in the lower Skoorsteenberg Formation of the Ecca Group. Of 13 total analyses, four were rejected based on high discordance. Nine individual zircon analyses yielded concordant U-Pb ages that range from 275 to 255 Ma. The youngest population consists of four grains that range from 264 to 255 Ma and yield a weighted average of 262.8 ± 3.8 Ma (MSWD = 0.49); the older population consists of five grains that range from 275 to 268 Ma and yield a weighted average of 271.6 ± 3.0 (MSWD = 0.40).

Sample 12ZA08

Sample 12ZA08 was collected ~175 m upsection from 12ZA10, from a ~1 cm thick, light green, clay-textured tuff interbedded in mudstones in the middle Skoorsteenberg Formation of the Ecca Group. Of 16 total analyses, 10 analyses yielded concordant ages. Carboniferous ages (309, 311 Ma) were produced from two discordant analyses, while the youngest ages were concordant and Permian–Triassic in age (270–252 Ma). The youngest population consists of five grains that range from 265 to 253 Ma and yield a weighted average of 256.5 ± 5.8 Ma (MSWD = 1.3). An older population of five grains ranges from 270 to 267 Ma and produces a weighted average of 267.8 ± 2.6 (MSWD = 0.22).

Sample 12ZA07

Sample 12ZA07 is from a 5 cm-thick, tan-to-green/grey tuff interbedded in mudstones near the base of the Kookfontein Formation of the Ecca Group, which conformably overlies the Skoorsteenberg Formation. Sample 12ZA07 is ~225 m stratigraphically above sample 12ZA08. Of the 18 zircon grains analysed, five were rejected due to discordance. From the 13 concordant ages, two anomalously old ages (539 and 294 Ma) were dismissed as inherited outliers, while 11 Permo-Triassic grains ranged from 273 to 237 Ma. The youngest five grains form a coherent population range from 254 to 237 Ma that produces a weighted average of 250.3 ± 4.8 Ma (MSWD = 1.0). An older population of six grains ranges from 273 to

259 Ma and yields a weighted average of 267.8 ± 5.9 (MSWD = 2.9).

Beaufort Group

Two tuffs were sampled from the Adelaide Subgroup of the Beaufort Group to augment four tuff ages from Lanci *et al.* (2013).

Sample 12ZA16

Sample 12ZA16 is from a 5 to 10 cm-thick, white, chalky tuff interbedded within mudstones in the lower Abrahamskraal Formation (Adelaide Subgroup) of the Beaufort Group. Of the 16 total analyses, 11 yielded concordant ages ranging from 291 to 256 Ma. One analysis yielded an age of 291 Ma and is considered to be an outlier, since it is 17 million years older than the next youngest age. The youngest coherent population of zircon yields a weighted average of 264.7 ± 2.5 Ma (MSWD = 0.86) from seven grains, with an older >270 Ma population of three grains that yields a weighted average of 271.8 ± 2.4 Ma (MSWD = 0.25).

Sample 12ZA18

Sample 12ZA18 is from a 45 cm-thick, white-to-green tuff in the upper Abrahamskraal Formation (Adelaide Subgroup) of the Beaufort Group, approximately ~50 m above 12ZA16. From 37 total analyses, 28 concordant ages were produced. Inherited, pre-Permian grains dominate the sample, with 17 concordant analyses ranging from 2607 to 359 Ma. Permian age grains range from 290 to 238 Ma. The two oldest Permian grains (286, 290 Ma) are dismissed as inherited outliers. The youngest populations of four grains range from 267–255, which yields a weighted average of 260.6 ± 8.9 (MSWD = 7.4). An older population of five grains ranges from 278 to 272 Ma and produces a weighted average of 274.5 ± 3.9 (MSWD = 1.4). Two older, Permian grains (286, 290 Ma) may represent a minor population, but are considered significantly older, inherited outliers. Two Triassic ages (238, 239 Ma) form a small population, but both analyses have elevated common Pb values.

Laingsburg depocentre: southwest basin

Because the Ecca Group tuffs were well characterized by Fildani *et al.* (2007, 2009), we sampled tuffs in the Adelaide Subgroup of the Beaufort Group from the Laingsburg subbasin (Figure 1B) and report four new tuff ages. Like the Tanqua section, tuffs are common throughout the strata; however, no tuffs were identified between the samples presented by Fildani *et al.* (2007, 2009) and 12ZA05.

Sample 12ZA05

Sample 12ZA05 was collected from an ~ 30 cm-thick, well-lithified, light-brown tuff within the upper Fort Brown Formation of the Ecca Group in the Laingsburg subbasin. Out of 18 total analyses, 14 grains produced concordant ages. Older, >300 Ma grains dominate this sample, since 13 of 14 concordant ages ranged from 2139 to 304 Ma. Only one analysis yielded a concordant Permian age of 274.3 ± 4.6 Ma.

Sample BLOU

Sample BLOU was collected from a well-lithified tuff interbedded in the Abrahamskraal Formation (Adelaide Subgroup) of the Beaufort Group. Of 26 total analyses, 22 grains produced concordant U-Pb ages. The tuff was dominated by older, >300 Ma grains, with 14 grains between ~3.2 Ga and 372 Ma. Of eight Permian grains ranging from 289 to 272 Ma, six grains were interpreted to form a coherent population ranging between 279 and 272 Ma that produced a weighted mean of 276.4 ± 2.3 (MSWD = 0.69).

Sample SUTH

Sample SUTH was collected from a well-lithified tuff interbedded in the Abrahamskraal Formation (Adelaide Subgroup) of the Beaufort Group. Of 32 total analyses, 22 grains produced concordant ages. An older group of eight concordant ages ranged between 1750 and 468 Ma, while 14 concordant Carboniferous–Permian ages ranged from 301 to 260 Ma. Two populations are interpreted from Permian ages: the youngest coherent population of six ages that range from 267 to 260 Ma and yields a weighted mean of 264.9 ± 1.9 Ma (MSWD = 1.17); an older, coherent population of four grains ranges from 276 to 270 Ma and yields a weighted mean age of 271.7 ± 2.3 Ma (MSWD = 1.17).

Sample 13ZA93

Sample 13ZA93 was collected from an ~25 cm-thick tuff interbedded between mudstones in the upper Abrahamskraal Formation (Adelaide Subgroup) of the Beaufort Group. Only eight zircon grains were separated and U-Pb analysis reveals that the zircon grains are largely recycled, since six of eight are >300 Ma. No coherent zircon population was interpreted from the two Permian grains (269, 280 Ma) present and the youngest grain, 269 Ma, is reported in Figure 4.

Prince Albert transect: south-central basin

Three samples were collected from the Lower Ecca Group in the central basin (Figure 1B), near Prince

Albert, Western Cape. This location is between the Laingsburg and Ripon subbasins. The strata here represent a condensed section, and no tuff gap is reported for this composite section, however this region has not been fully logged or studied in detail. These data augment work by Rubidge *et al.* (2013), who reported ID-TIMS zircon U-Pb ages from tuffs within the Adelaide and Tarkastad Subgroups of the Beaufort Group ~100 km to the north.

Sample 12ZA19

Sample 12ZA19 was collected from a light-green ash ~8 m above the base of the Prince Albert Formation of the Ecca Group. Of 19 zircon grains that were analysed, 11 concordant ages were produced. Concordant, inherited zircon ages were 526, 542, and 642 Ma, while eight Permian, concordant zircon ages range from 281 to 272 Ma. Two populations of zircon are interpreted from concordant ages with the youngest population of six grains that range from 277 to 272 Ma and yield a weighted average of 273.7 ± 2.7 Ma (MSWD = 0.37), with two older ~280 Ma grains (280, 281 Ma) treated as outliers.

Sample 12ZA22

Sample 12ZA22 was collected from a brown, fissile ash near the base of the Ripon Formation of the Ecca Group. This ash yielded zircon that produced 13 concordant ages from 18 analyses. Concordant, inherited zircon ages ranged from 432 to 1018 Ma (n = 7), while six Permian-Triassic, concordant zircon ages range from 266 to 248 Ma. Two populations of zircon are interpreted from concordant ages: the youngest population of four grains ranges from 259 to 248 Ma and yields a weighted average of 255.1 ± 4.5 (MSWD = 0.76) Ma. An older ~265 Ma population is represented by two grains (266, 264 Ma) that are treated as outliers.

Sample 12ZA23

Sample 12ZA23 was collected from a soft, green, clay-rich ash in the Ripon Formation of the Ecca Group. Of 34 grains analysed, 30 analyses yielded concordant, Permian-Triassic ages that range from 249 to 283 Ma. A single, concordant 470 Ma age was also produced. Based on a histogram of concordant Permo-Triassic ages, age spectra peaks occur at ~282 Ma, ~271 Ma, ~266 Ma, 258 Ma, and 250 Ma. A population of seven zircon grains has concordant age ranges from 249 to 257 Ma and yields a weighted average of 251.1 ± 2.5 Ma (MSWD = 1.07). Grouping of the 20 older Permian analyses results in a weighted average of 267.3 ± 1.3 (MSWD = 0.91).

Ripon depocentre: eastern basin

Nine samples were collected from the Ripon depocentre in the eastern Karoo Basin: four from the Ecca Group and five from the Adelaide Subgroup of the Beaufort Group. All nine samples are from a single continuous, N-dipping section exposed in roadside outcrops and represent the first geochronology in the eastern basin (Figure 1B). No volcanic deposits were found in the interval between sample 12ZA61 in the upper Ecca Group and 12ZA46 in the Lower Beaufort Group. The rest of the strata contained numerous tuff beds interbedded throughout the strata.

Sample 12ZA54

Sample 12ZA54 was collected from a brown, clay-rich ash about 1.5 m below the top of the Collingham Formation of the Ecca Group. Of 16 total zircon analyses, 10 grains yielded concordant ages. The oldest ages (458, 456, 431 Ma) were produced from concordant analyses, while the youngest, concordant, Permian–Triassic ages range from 277 to 257 Ma. A coherent population of five zircon grains ranges from 269 to 257 Ma and produces a weighted average of 263.1 ± 6.4 Ma (MSWD = 1.4). Two inherited Permian grains of 271 and 277 Ma are treated as outliers.

Sample 12ZA55

Sample 12ZA55 was collected from a green, clay-rich ash approximately 6 m above the base of the Collingham Formation. From 18 total zircon analyses, nine grains produced concordant ages. A single inherited zircon produced a concordant age of 341 Ma, while eight grains produced concordant, Permian ages that range from 291 to 259 Ma. One population of zircon is interpreted from six concordant ages that range from 269 to 259 Ma and yields a weighted average of 268.0 ± 3.2 Ma (MSWD = 1.4).

Sample 12ZA60

Sample 12ZA60 was collected from a clay-rich, white-to-tan ash within the Ripon Formation of the Ecca Group. Of 16 total zircon analyses, 14 concordant ages were produced. The oldest ages (450, 351 Ma) were produced from concordant analyses, while the younger, concordant, Permian ages (n = 12) range in age from 295 to 257 Ma. Two populations of zircon are interpreted from concordant ages; the youngest population of five grains ranges from 264 to 257 Ma and yields a weighted average of 262.5 ± 3.0 Ma (MSWD = 0.21), while an older population of six grains yields a weighted average age of 268.7 ± 1.8 (MSWD = 0.92).

Sample 12ZA61

Sample 12ZA61 was collected within a clay-rich ash within the Lower Fort Brown Formation of the Ecca Group. Of 25 total analyses, 21 zircon grains produced concordant ages. Older, inherited ages (516, 520, 1108 Ma) were produced from concordant analyses, while younger, Permian–Triassic, concordant ages range in age from 274 to 232 Ma. A significant late Permian to middle Triassic population was resolved in this sample; however three of the analyses have high uncertainties, making them less reliable than high-precision analyses but still meaningful. Two populations of zircon are interpreted from concordant ages; the youngest population of eight grains ranges from 257 to 232 Ma and yields a weighted average of 251.6 ± 3.9 Ma (MSWD = 2.8), while an older population of 10 grains ranges from 274 to 257 Ma and produces a weighted average of 264.7 ± 3.2 Ma (MSWD = 1.9).

Sample 12ZA46

Sample 12ZA46 was collected from an ash within the Koonap Formation (Adelaide Subgroup) of the Beaufort Group. Only 11 zircon grains were recovered from this sample. All 11 grains were analysed, however only nine produced concordant ages. Older, inherited ages (325, 464, 478, 523 Ma) were produced from concordant analyses, while younger, Permian concordant ages range from 285 to 253 Ma, excluding a concordant 229 Ma analysis with high common-Pb. One population of zircon is interpreted from concordant ages that range from 260 to 253 Ma and yields a weighted average of 257.3 ± 4.3 Ma (n = 4), with a single 285 Ma grain treated as a statistical outlier.

Sample 13ZA75A

Sample 13ZA75 was collected from a brown, gritty ash within the Koonap Formation (Adelaide Subgroup) of the Beaufort Group. Of 15 total analyses, only eight grains yielded concordant ages. Older, inherited ages (431, 469, 505, 584, 1112 Ma) were produced from concordant analyses, while three younger, concordant Permian ages are scattered at 265, 270, and 278 Ma. No distinct zircon population is interpreted from this sample, and a weighted mean age of the three Permian zircon is 270 ± 15 Ma.

Sample 13ZA76

Sample 13ZA76 was collected from a white, chalky ash within the upper Koonap Formation. Of 40 total analyses, 31 grains produced concordant ages. Inherited, pre-Permian grains range from 1721 to 326 Ma (n = 6). Two populations are interpreted from Permian ages, with the youngest population of eight grains producing an age of 260.4 ± 2.8 Ma (MSWD = 1.9), while a 267.6 ± 1.5 Ma age (MSWD = 0.84) is interpreted as an inherited population.

Sample 12ZA45

Sample 12ZA45 was collected from an ash interbedded in a mudstone-rich interval of the uppermost Koonap Formation of the Beaufort Group. Only nine zircon grains were recovered from this sample, all of which were analysed. Six grains produced concordant ages. Additional analysis was hampered due to a low abundance of zircon in this sample. Older, inherited concordant ages (445, 454, 455, 457, 522, 1098 Ma) dominate the zircon population, with the only younger age (271 Ma) excluded due to high discordance. The four Ordovician zircon grains form a tight cluster, and yield a 452.5 ± 9.5 Ma (MSWD = 2.7) weighted average age.

Sample 13ZA72A

Sample 13ZA72 was collected from a white, chalky-textured ash within the Middleton Formation (Adelaide Subgroup) of the Beaufort Group. Of 32 total analyses, 28 grains produced concordant ages. Concordant, pre-Permian ages (n = 11) range from 1102 to 334 Ma, and concordant Permian zircon grains range between 282 and 252 Ma (n = 17). Two coherent populations are interpreted: the youngest population of four grains ranges from 258 to 252 Ma and produces a weighted mean age of 255.3 ± 4.0 (MSWD = 1.3), and the older, inherited population of five grains yields an age of 267.8 ± 3.6 Ma (MSWD = 1.4).

Discussion

Tuff distribution and composition-Gondwanan tuff gap

The abundant tuffs interbedded throughout the Karoo Supergroup strata provide the opportunity to assess U-Pb zircon ash ages from numerous stratigraphic horizons over an ~2–3 km thick section and offer insight into the Karoo Basin evolution. Based on field observations, the three major depocentres, Tanqua, Laingsburg, and Ripon, all contain a stratigraphic interval where tuffs are not present. We note that the textural character of air-fall tuffs is, in general, different above and below this observed gap in tuff deposition. Below the gap, tuffs are green, clay-rich, and typically <10 cm. In contrast, above the gap, tuffs are distinctly either white and chalky or light brown and gritty/sandy with thicknesses varying from 5 cm up to 40 cm. We speculate here that this ‘tuff gap’ is similar to the ‘tuff gaps’ reported throughout southern Gondwana (New Zealand, Australia, and Antarctica), where volcanic tuffs are rare to absent within otherwise ash-rich strata (Veevers *et al.* 1994b). It remains

unclear whether those tuff gaps are related to a hiatus in volcanic activity or dilution and lack of preservation in a terrestrial depositional environment (Retallack and Krull 1999; Veevers 2004); these gaps, however, are thought to be synchronous across Gondwana (Veevers 2004). We propose herein an unidentified tuff gap in the Karoo strata that is present in a variety of depositional environments, recorded in deep-to-marginal marine (Ecca Group) and terrestrial (Beaufort Group) sediments across the basin (Figures 3 and 4). Although the cause of the tuff gap is still poorly understood and the mechanism responsible for the evolution from clay-rich to chalky and gritty/sandy tuffs is unknown, these observations provide a distinct framework with three distinct ash regimes: green, clay-rich tuffs; ash absent altogether (i.e. tuff gap); and chalky/gritty tuffs.

The appearance and character of the Karoo tuffs might be due to either (1) a change in weathering conditions; (2) dilution of tuffs with clastic detritus; or (3) evolution of the volcanic ejecta from glass-dominated tuffs preserved as clay-rich tuffs to lithic deposits, manifesting as chalky or gritty/sandy tuffs. Since tuffs occur above this tuff gap, in both marginal marine and terrestrial strata deposited in both high- and low-energy environments, it is unlikely the ash regimes are due to clastic dilution. Additionally, the tuff gap is typically present in deep to marginal marine low-energy depositional environments where dilution would be unlikely. Tuffs above the gap also generally contain smaller zircon populations (<100 zircons kg^{-1}) than tuffs below (≫100 zircons kg^{-1}). During mineral separation, the heavy mineral composition of chalky and gritty tuffs was found to commonly contain dark, lithic grains, while clay-rich tuffs yielded few to no lithic grains and were dominated by mineral grains in the heavy mineral separates. This suggests that tuffs below the tuff gap may have been crystal-rich vitric tuffs, while the overlying volcanics are likely zircon-sparse, lithic tuffs.

Maximum depositional ages from U-Pb zircon analyses

Based on these new U-Pb zircon SHRIMP results, integrated with previously published data (Coney *et al.* 2007; Fildani *et al.* 2007, 2009; Lanci *et al.* 2013; Rubidge *et al.* 2013), (Figures 3 and 4) strata of the Ecca Group below the regional tuff gap appear coeval across the southern margin of the basin based on ash ages, with the base of the Ecca Group ~275 Ma, and consistent younging upward stratigraphically across the basin (Figure 5A) to the base of the ash gap at ~250 Ma, above which volcanic tuffs become rare to absent for ~300–600 m. Tuffs in the Beaufort Group above this interval consistently yield ages older than the underlying strata and do not display a younging-upward trend (Figure 5B). Fildani *et al.* (2007, 2009) and Lanci *et al.* (2013) presented tuff ages based on extensive SHRIMP datasets (N = 16, n = 205 and N = 4, n = 111, respectively) to address the absolute age of the strata. Fildani *et al.* (2007, 2009) only presented ages from the Ecca Group, while Lanci *et al.* (2013) only presented data from the overlying Beaufort Group. When compared to limited data that were available at the time, Coney *et al.* (2007) and Fildani *et al.* (2009) observed a discrepancy in the ages of the Ecca and Beaufort Groups and used those ages to present a model for time-transgressive filling across the basin. Lanci *et al.* (2013) suggested that the robust single crystal age data presented by Fildani *et al.* (2007, 2009) were erroneously young due to Pb-loss. The ages presented in this study are based on zircon age populations ($n \geq 3$) to estimate ash ages, greatly minimizing the chances of the age being affected by Pb-loss (Saylor *et al.* 2012), but corroborate, support, and reproduced the age estimates produced by Fildani *et al.* (2007, 2009), Coney *et al.* (2007), Weislogel *et al.* (2011), Lanci *et al.* (2013), and Rubidge *et al.* (2013). It is not likely that the zircon ages presented in this study have been affected

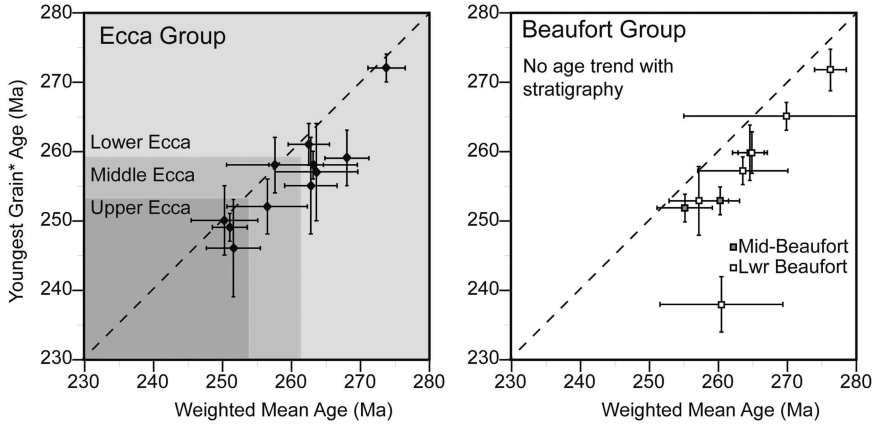

Figure 5. Youngest grain age (Ma) vs. weighted mean age (Ma) plot (left) shows a younging upsection of U-Pb zircon tuff ages in the Ecca Group. In the Beaufort Group (right), no trend is observed. Two samples (13ZA72A-Middleton Fm, 13ZA76-Upper Koonap Fm) in the Middle Beaufort produce ages that are within error one of the lowest stratigraphic samples (12ZA46-an ash located directly above the 'tuff gap' in the Lower Koonap Fm). No younging-upward trend however is observed in the Beaufort Group tuffs.

by Pb-loss because (1) only concordant analyses were considered; (2) ash ages are based on concordant age populations and weighted averages; (3) individual results are repeatable (Fildani *et al.* 2007, 2009; Lanci *et al.* 2013; Rubidge *et al.* 2013); and (4) the observed age inversion is present in both this study and previous studies (Fildani *et al.* 2007, 2009; Coney *et al.* 2007; Weislogel *et al.* 2011; Lanci *et al.* 2013; Rubidge *et al.* 2013) using a variety of analytical techniques (SHRIMP, TIMS, LA-ICPMS) and consistently occurs across the basin directly above the proposed tuff gap. No relationship between U concentration and age was observed, further suggesting that Pb-loss from U-decay, lattice damage, and diffusion has not affected concordant zircon ages (Kryza *et al.* 2012). If Pb-loss is attributed to be the cause of the observed contradictory ages, then it must be more significant and pervasive in the Ecca Group than in the Beaufort Group, which would require a stratigraphically selective Pb-loss mechanism that disturbed the isotopic systems of some tuffs, while leaving others in the overlying strata effectively unaltered. Therefore, we interpret the weighted mean U-Pb zircon ages to represent a maximum depositional age of the air-fall ash and will explore the implications of these new age controls across the >600 km-long southern margin of the Karoo Basin.

The abrupt appearance of older ages is restricted to the strata above the observed tuff gap. Possible mechanisms that could cause these older, seemingly anomalous tuff ages include the following: (1) structural juxtaposition of older strata (fluvial) over younger (marine); (2) time-transgressive facies tracts producing synchronous marine and terrestrial deposition; (3) detrital reworking and contamination in high-energy, terrestrial environments; and (4) lack of co-eruptive zircon in early-to-mid Triassic tuffs.

No field evidence by any workers in the Karoo Basin has been observed or reported to identify tectonic structures that could render older-over-younger strata over thousands of square kilometres to cause inversion of zircon ages in the tuffs. Tanqua depocentre strata are flat lying and undeformed and Beaufort and Ecca Group strata in the Laingsburg and Ripon depocentre are deformed by broad, upright folds; any repetition of mapped strata is locally isolated.

Alternately, time-transgressive facies deposition could create the observed age inversion. Previous models for basin infilling based on palaeoflow and provenance analysis concluded that sediment was transported into the basin mainly from the south; this model would predict stratigraphic younging of ash beds northward (Veevers *et al.* 1994a; Rubidge 2000; Flint *et al.* 2011). However, this scenario appears to conflict with the observed older zircon ages in Beaufort Group tuffs that lie to the north of the younger Ecca Group ash samples. Fildani *et al.* (2009) suggested diachronous filling of the basin from east to west, with terrestrial deposition in the east being coeval with deep marine conditions in the west. The new results from the Ripon depocentre indicate contemporaneous marine deposition over >600 km across the southern margin of the Karoo Basin and do not support this scenario unless we hypothesize a highly segmented basin. Recent studies of the Beaufort Group (Lanci *et al.* 2013; Wilson *et al.* 2014) report consistent palaeocurrents to the northeast, supporting a sediment dispersal pattern for the whole deep water to fluvial section. For diachronous filling to produce the observed age inversion, marine conditions in the southern basin would need to be coeval with or post-date fluvial deposition to the north. While no evidence in the stratigraphic record has been directly identified to support either of these scenarios, more age constraints from across the basin are required to better understand basin-wide sedimentation patterns.

Here, we consider the possibility that some tuffs within the Karoo Supergroup do not contain coherent populations of terminal-phase, co-eruptive zircon. In this scenario, a terminal-phase zircon population may be present, but is diluted by older zircon due to (1) sedimentary reworking of older ash or clastic material within younger ash deposits; (2) inclusion of older xenocrystic or comagmatic zircon residing within the magmatic system; or (3) incorporation of older lithic volcanic material from the volcanic carapace during eruption. One Beaufort Group ash sample (12ZA46) showed signs of detrital contamination, with 5 of 10 zircon grains being significantly older (>280 Ma) than the youngest coherent population (257.3 ± 4.3 Ma; $n = 4$). Air-fall tuffs deposited in fluvial depositional environments, such as the Beaufort Group depositional system, are particularly prone to reworking and detrital mixing by overland flows, pedogenesis, and bioturbation. While it is difficult to assess the role of clastic dilution and terrestrial reworking without resolving the detrital zircon populations of adjacent siliciclastic units, tuffs within the Beaufort Group retain an ash lithology and show no physical signs of detrital reworking. If tuffs were significantly contaminated with detrital zircon, that would require significant reworking with a large volume of clastic material such that the ash lithology would not be retained.

In addition, with nine ash ages for the Beaufort from this study and four tuffs from Lanci *et al.* (2013), 113 grains yield a Permian age, yet only four moderately concordant Triassic grains have been recovered (12ZA18 shown in Figure 6G), compared to 253 concordant Permian grains and 26 concordant Triassic grains in the 13 age tuffs within the Ecca Group from this study and eight tuffs from Fildani *et al.* (2007, 2009). Of the 26 concordant Triassic ages in the Ecca Group, 18 were obtained from tuffs just below the presumed tuff gap (12ZA07, CVX12, 12ZA23, 12ZA61). These four samples all yield ~250–251 Ma weighted mean ages, which coincides with the basal age of the tuff gap (~251 Ma)

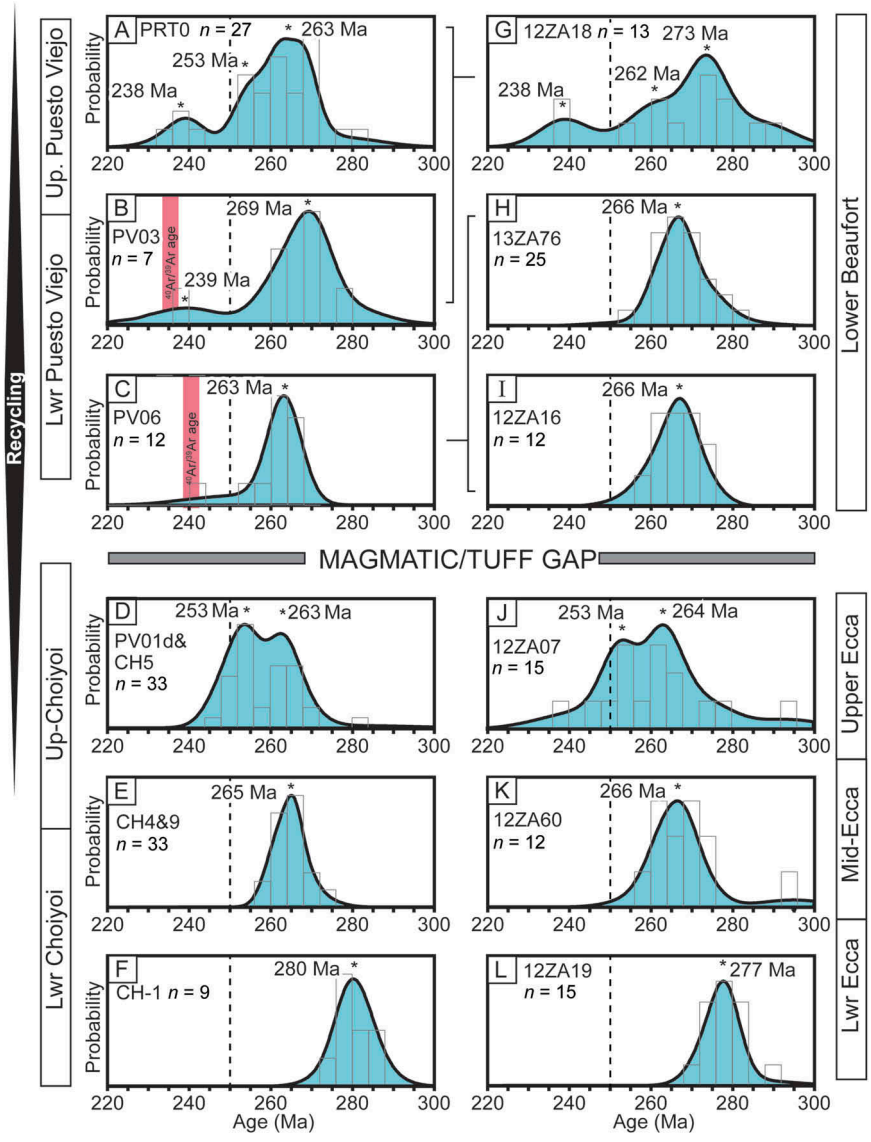

Figure 6. Correlation of KDE plots from the Puesto Viejo (A, B, C) and Choiyoi (D, E, F) volcanic suites to comparable KDE signatures in interbedded tuffs of the Karoo Supergroup. Beaufort Group (G, H, I) samples show similar KDE signatures to the Puesto Viejo volcanics, while the underlying Ecca Group samples (J, K, L) match the stratigraphic trend observed in the Choiyoi Group. The uppermost Choiyoi samples contain peaks at 253 and 263 Ma, compared to 253 and 264 Ma in the Ecca Group directly below the base of the tuff gap.

elsewhere in Gondwana (Veevers *et al.* 1994b). Since the base of the tuff gap is approximately the boundary between the Permian and Triassic, ages just below this interval would be expected to straddle the boundary, with a range of ~249–254 Ma ages, which is observed in Ecca tuffs and is compatible with our age interpretation. Furthermore, the absence of a large, Triassic zircon population in Beaufort tuffs suggests limited availability of co-eruptive, autocrystic zircons in the Beaufort Group. Magmatic recycling is also compatible with the observation of shared recycled populations within the weighted averages of ash zircon populations, where seven tuffs in this study contained an ~267–268 Ma tuff population (P_1 of 12ZA16, 12ZA55, SUTH, and P_2 of 12ZA23, 12ZA60, 13ZA72, 13ZA76) and seven tuffs contained an ~261–264 Ma tuff population (P_1 of 12ZA10, 12ZA18, 12ZA54, 12ZA60, 13ZA67, 13ZA76, and P_2 of 12ZA61). These inherited populations likely represent zircon crystallization events in the magmatic source of the tuffs and may be present in any subsequently erupted ash. A similar observation has been made in proximal volcanic deposits in the Southern Pyrenees, where distinct zircon crystallization events are represented in subsequent eruption events (Pereira *et al.* 2014). Recycling is further

suggested by the dominance of 25 concordant Ordovician xenocrysts in Karoo tuffs from this study alone, which is most evident in sample 12ZA45, where the only coherent age population (n = 4 of 6 concordant analyses) consisted of ~453 Ma grains.

Recycling of antecrystic and xenocrystic zircon in late Permian–Triassic volcanics is recognized in correlative volcanics in South America (Spalletti *et al.* 2008; Domeier *et al.* 2011). Two successive magmatic suites in South America, the Permian Choiyoi Group and Triassic Puesto Viejo Group, record the same volcanism responsible for tuffs in the Karoo Supergroup. The Permian Choiyoi Group yields well-defined U-Pb zircon age peaks between 280 and 253 Ma (Figure 6D–F) with signs of zircon recycling restricted to the uppermost Upper Choiyoi Group. A tuff from the Upper Choiyoi was found to be dominated by ~276 Ma zircon (SM-1; Rocha-Campos *et al.* 2006) and also contains a distinct subpopulation of ~253 Ma zircon (n = 4; Rocha-Campos *et al.* 2006). This ~253 Ma age reflects the age of the last phases of Choiyoi volcanism (Kleiman and Japas 2009). Zircon recycling intensifies within the Triassic Puesto Viejo Group, which contains more complex zircon populations (Figure 6A–C). Published U-Pb zircon from the lowest Puesto Viejo Group (PV06 of Domeier *et al.* 2011; PRT0 of Spalletti *et al.* 2008; from the Potrerillos Fm, a coeval, stratigraphic equivalent of the Puesto Viejo Group [Ottone *et al.* 2014]) shows that samples contain dominant ~260–280 Ma populations with few to no Triassic grains. $^{40}Ar/^{39}Ar$ feldspar ages for the same intervals range between 239 and 235 Ma, suggesting a >20 million-year discrepancy between U-Pb zircon and $^{40}Ar/^{39}Ar$ feldspar geochronology systems. Samples from the mid-to-upper Puesto Viejo Group contained significantly more Triassic grains (PRT1, PRT2 of Spalletti *et al.* 2008; Ottone *et al.* 2014), yielding weighted mean ages of 239–230 which are within error of correlative $^{40}Ar/^{39}Ar$ feldspar ages. The high proportion of Permian grains and discrepancies between U-Pb zircon and $^{40}Ar/^{39}Ar$ ages in the lowest Puesto Viejo Group led Domeier *et al.* (2011) to suggest that these volcanics were dominated by recycled, xenocrystic zircon. These observations were further used to propose that the Puesto Viejo magma chamber was volumetrically too small to generate new zircon grains (Domeier *et al.* 2011).

When U-Pb zircon spectra from Karoo Supergroup tuffs (Figure 6G–L) are compared to age-equivalent volcanics in South America (Figure 6A–F), the impact of zircon recycling on tuff geochronology can be observed. Lower Choiyoi volcanic samples (Figure 6E–F; Rocha-Campos *et al.* 2011) contain a single, cohesive zircon population, which was resolved in samples from the lower–middle Ecca Group. Samples from the uppermost Upper Choiyoi (PV01d from Domeier *et al.* 2011; CH-05 from Rocha-Campos *et al.* 2011; SM-1 from 2006-data unpublished), however typically contain a late Permian zircon population (~253 Ma) that is distinct from older middle-to-late Permian populations (~263–273 Ma). The KDE for available data from the uppermost Upper Choiyoi volcanics (Figure 6D) is remarkably similar to Upper Ecca Group tuffs (Figure 6J), with local maxima at ~253 and ~263 Ma. Comparison of U-Pb zircon and $^{40}Ar/^{39}Ar$ ages (Figure 6B, C) for the Lower Puesto Viejo volcanics demonstrate that Early to Middle Triassic volcanics do not contain dominant, co-eruptive zircon populations, but are rich in older, mid-Permian zircon (Figure 6C). This trend is observed in samples from the Lower Beaufort (Figure 6H, I). In subsequent Puesto Viejo volcanics, small, coherent populations of co-eruptive zircon become observable (Figure 6A, B), which can also be observed in zircon populations from Lower Beaufort tuffs (Figure 6G). Based on the similarity of zircon population distributions, weighted mean ages, and stratigraphic position relative to the overlying magmatic/tuff gap, we propose several age correlations (Figure 7).

(1) Lowest Ecca Group tuffs (within the Prince Albert, Whitehill Formations) are age equivalent to the early–middle Permian Lower Choiyoi Group (>265 Ma).
(2) Mid-Ecca Group tuffs (within the Collingham, Vischkuil, Skoorsteenberg, Laingsburg, Ripon Formations) are age equivalent to the upper, Lower Choiyoi and lowest Upper Choiyoi Group rocks (~265–255).
(3) Upper Ecca Group tuffs (Kookfontein, Fort Brown Formations) are age equivalent to the late Upper Choiyoi Group (253 Ma).
(4) The overlying Lower Beaufort Group tuffs are dominated by recycled zircon grains, which suggest they are age equivalent with Puesto Viejo volcanism (241–235 Ma).
(5) The tuff gap proposed in this study (Figures 3, 4, 7) could represent magmatic quiescence between Choiyoi and Puesto Viejo magmatic activity (252–241 Ma).

Implications for magmatism in southern Gondwana

Zircon is known to be present in variable concentrations in different tectonographic terranes (discussed as 'zircon fertility' in Moecher and Samson 2006). Therefore a zircon-rich terrane would be overrepresented in any zircon geochronology study compared to a zircon-sparse or zircon-poor terrane. This is most commonly applied to understand the geologic bias in detrital zircon provenance studies. The same mechanism, however, may create bias in the study of a magmatic system if certain magmatic systems produce few to no zircon, while others generate large volumes of zircon. The Southern Gondwanan magmatic system as recorded in

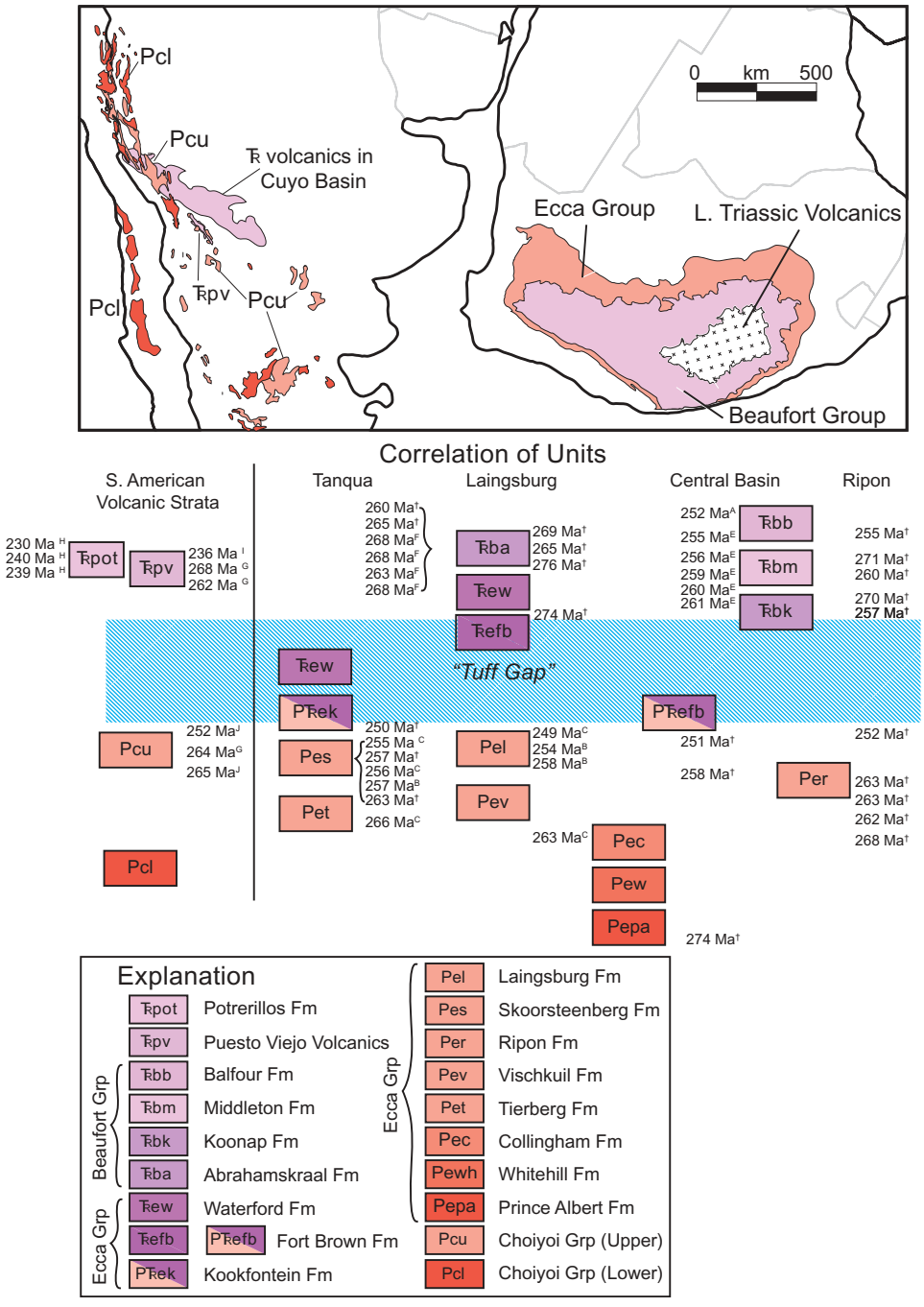

Figure 7. Simplified Geologic Map of the Choiyoi Group (Upper and Lower), Puesto Viejo Volcanics and coeval equivalents (Potrerillos Fm), and Karoo Supergroup, with a detailed correlation of units showing time equivalent stratigraphy and relevant age controls from Figure 3. South American geology from Spalletti *et al.* (2008), Kleiman and Japas (2009), and Ottone *et al.* (2014).

South America and the Karoo Basin appears to have consisted of three distinct pulses of magmatism: (1) zircon-rich, subduction and orogenic collapse driven magmatism that erupted crystalliferous, vitric tuffs prior to ~252 Ma; (2) magmatic and volcanic quiescence from 252 to 241 Ma; and (3) renewed magmatism driven by extensional rifting that resulted in recycling of older crustal materials and eruption of lithic tuffs. Crystalline basement rocks from the Antarctic Peninsula (Riley *et al.* 2012), which would have been tectonically adjacent to South Africa within Gondwana (Figure 1A), provide further insight into zircon crystallization over

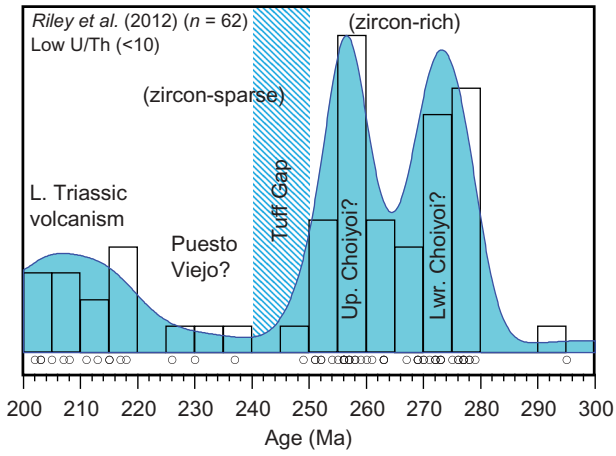

Figure 8. KDE age distribution of igneous (U/Th < 10) Permian–Triassic zircon from Gondwanan crystalline basement in the Antarctic Peninsula (Riley *et al.* 2012). The peaks of zircon ages represent pulses of igneous zircon crystallization. Two peaks at ~272 and ~255 Ma are coeval with Lower and Upper Choiyoi volcanism, no zircon is found in the time interval of the tuff gap, and a few, sparse zircon grains correlate to Puesto Viejo volcanism, despite known Early Triassic volcanism in Southern Gondwana.

time (Figure 8). Permian–Cretaceous basement from the Antarctic Peninsula contains co-emplacement and recycled igneous zircon, as well and metamorphic zircon that records Permian–Triassic metamorphism. When considering only low U/Th (<10; n = 62), which likely represents igneous zircon (Hoskin and Black 2000), there is a distinct pattern that is strikingly similar to the zircon trends observed in South America and South Africa. There are two Permian spikes of zircon represented in the Antarctic samples at ~272 and ~255 Ma. They roughly correlate to the Lower (290–265 Ma) and Upper (270–250 Ma) Choiyoi Group volcanic suites and the latter pulse with the tuffs of the Ecca Group. Only one zircon lies within the range of the tuff gap, but this grain also is within error or the ~255 Ma peak; therefore, there are effectively no zircon grains produced during this interval, which likely reflects magmatic quiescence. The Antarctic Peninsula samples only yield three grains that correlate with Puesto Viejo magmatism (240–220 Ma). Despite known volcanism during this time, the sparse presence of such a small population suggests that very few zircon grains were crystallized during this period. These observations, along with the lack of co-eruptive zircon in South American and Karoo Basin volcanics, strongly suggest that zircon production in Southern Gondwana was subdued in the Early Triassic across the western half of the margin. The lack of co-eruptive zircon, therefore, may be a super-regional phenomenon that might affect more areas throughout Gondwana, particularly in the Early Triassic, thereby hindering U-Pb zircon geochronology in Early Triassic volcanics.

Summary

Using 469 new single-grain analyses, we used coherent age populations to determine 22 U-Pb zircon tuff ages in four stratigraphic sections of the lower Karoo Supergroup across the Karoo Basin. Regionally, tuffs within the terrestrial Beaufort Group consistently produce ages that are older than the underlying marine Ecca Group, which can be observed in multiple studies (Coney *et al.* 2007; Fildani *et al.* 2007, 2009; Lanci *et al.* 2013; Rubidge *et al.* 2013) using different analytical techniques (SHRIMP, TIMS, LA-ICP-MS). The reproducibility of tuff ages in the marine section and internally consistent age for the base of the tuff gap suggests that tuffs below a proposed regional tuff gap may provide reliable chronostratigraphic control, while tuffs above the tuff gap yield chaotic ages that predate deposition (Figure 5). We propose that post-depositional reworking combined with a lack of terminal phase, volcanic zircon in distal air-fall tuffs within the Beaufort Group may be responsible for the inversion of U-Pb zircon ages. Zircon recycling is observed in correlative proximal volcanic tuffs in Permo-Triassic basins of South America corroborating this hypothesis. The zircon U-Pb ages from tuffs in the Beaufort Group should therefore be considered as constraints on maximum depositional ages, not as a representation of the actual depositional age (i.e. 'golden spike' ages). Our proposed explanation brings together data considered thus far puzzling and contradictory, and is compatible with recent observations in other long-lived arc to post-orogenic systems that show protracted zircon recycling (Pereira *et al.* 2014). Our observations support recent evidence from South America that the absolute ages assigned to Gondwanan biozones may be erroneously old (Ottone *et al.* 2014). Our new data are in agreement with all recently published ages (Fildani *et al.* 2007, 2009; Lanci *et al.* 2013; Rubidge *et al.* 2013) and demonstrate the importance of considering the magmatic history of a volcanic source when interpreting U-Pb zircon datasets from tuffs to estimate maximum depositional ages. These new data illustrate how tuff geochronology can, at times, be ambiguous when using a limited dataset. By compiling a regionally extensive study and understanding the nature of volcanism, however, the ambiguity might be reduced, resulting in more competent stratigraphic age controls.

Acknowledgements

Analytical support was provided by Dr Matt Coble of the Stanford University/USGS SUMAC SHRIMP Lab. This manuscript was greatly improved by reviews from Dr E.G. Ottone, Dr Brian Romans, an anonymous reviewer, Kathleen Kingry, and Dr Angela Hessler.

Disclosure statement

No potential conflict of interest was reported by the author(s).

Funding

Funding was provided through grants from West Virginia University, American Association of Petroleum Geologists, Society for Sedimentary Geology, Geological Society of America, and Dr R. Shumaker to McKay and Weislogel.

ORCID

Matthew P. McKay http://orcid.org/0000-0002-7756-6489
David M. Hodgson http://orcid.org/0000-0003-3711-635X

References

Barth, A.P., and Wooden, J.J., 2006, Timing of magmatism following initial convergence at a passive margin, southwestern U.S. Cordillera, and ages of lower crustal magma sources: The Journal of Geology, no. 114, p. 231–245. doi:10.1086/499573

Black, L.P., and others, 2004, Improved 206Pb/238U microprobe geochronology by the monitoring of a trace-element-related matrix effect; SHRIMP, ID–TIMS, ELA–ICP–MS and oxygen isotope documentation for a series of zircon standards: Chemical Geology, no. 205, p. 115–140. doi:10.1016/j.chemgeo.2004.01.003

Bouma, A.H., and Wickens, H.D., 1994, Tanqua Karoo, ancient analog for fine-grained submarine fans, *in* Weimer, P., Bouma, A.H., and Perkins, B.F. eds., Submarine fans and turbidite systems: sequence stratigraphy, reservoir architecture, and production characteristics SEPM, Gulf Coasts Section, 15th Annual Research Conference, p. 23–34.

Bowring, S.A., and Schmitz, M.D., 2003, High precision zircon geochronology and the stratigraphic record Hanchar, J.M., and Hoskins, P.W.O. Zircon: Experiments, isotopes, and trace element investigations: Reviews in Mineralogy and Geochemistry, no. 53, p. 305–326. doi:10.2113/0530305

Castiñeiras, P., Díaz García, F., and Gómez Barreiro, J., 2010, REE-assisted U–Pb zircon age (SHRIMP) of an anatectic granodiorite: Constraints on the evolution of the A Silva granodiorite, Iberian allochthonous complexes: Lithos, no. 116, p. 153–166. doi:10.1016/j.lithos.2010.01.013

Catuneanu, O., Hancox, P.J., Cairncross, B., and Rubidge, B.S., 2002, Foredeep submarine fans and forebulge deltas: Orogenic off-loading in the underfilled Karoo Basin: *Journal of African Earth* Sciences, no. 35, p. 489–502. doi:10.1016/S0899-5362(02)00154-9

Coleman, D.S., Gray, W., and Glazner, A.F., 2004, Rethinking the emplacement and evolution of zoned plutons: Geochronologic evidence for incremental assembly of the Tuolumne Intrusive Suite, California: Geology, no. 32, p. 433–436. doi:10.1130/G20220.1

Compston, W., and Gallagher, K., 2012, New SHRIMP zircon ages from tuffs within the British Palaeozoic stratotypes: Gondwana Research, no. 21, p. 719–727. doi:10.1016/j.gr.2011.11.010

Coney, L., and others, 2007, Geochemical and mineralogical investigation of the Permian-Triassic boundary in the continental realm of the southern Karoo Basin, South Africa: Palaeoworld, no. 16, p. 67–104. doi:10.1016/j.palwor.2007.05.003

Crowell, J.C., 1978, Gondwanan glaciation, cyclothems, continental positioning, and climate change: American Journal of Science, no. 278, p. 1345–1372. doi:10.2475/ajs.278.10.1345

Dickinson, W.R., and Gehrels, G.E., 2008, Sediment delivery to the cordilleran foreland basin: Insights from U-Pb ages of detrital zircons in Upper Jurassic and Cretaceous strata of the Colorado Plateau: American Journal of Science, no. 3084, p. 1041–1082.

Domeier, M., Van Der Voo, R., Tomezzoli, R.N., Tohver, E., Hendriks, B.W.H., Torsvik, T.H., Vizan, H., and Dominguez, A., 2011, Support for an "A-type" Pangea reconstruction from high-fidelity late Permian and early to middle Triassic paleomagnetic data from Argentina: Journal of Geophysical Research, no. 116B12114, p. 26. doi:10.1029/2011JB008495

Fildani, A., Drinkwater, N.J., Weislogel, A., McHargue, T., Hodgson, D.M., and Flint, S.S., 2007, Age controls on the Tanqua and Laingsburg deep-water systems: New insights on the evolution and sedimentary fill of the Karoo Basin, South Africa: Journal of Sedimentary Research, no. 77, p. 901–908. doi:10.2110/jsr.2007.088

Fildani, A., Weislogel, A., Drinkwater, N.J., McHargue, T., Tankard, A., Wooden, J., Hodgson, D., and Flint, S., 2009, U-Pb zircon ages from the southwestern Karoo Basin, South Africa-implications for the Permian-Triassic boundary: Geology, no. 37, p. 719–722. doi:10.1130/G25685A.1

Flint, S.S., and others, 2011, Depositional architecture and sequence stratigraphy of the Karoo basin floor to shelf edge succession, Laingsburg depocentre, South Africa: Marine and Petroleum Geology, no. 28, p. 658–674. doi:10.1016/j.marpetgeo.2010.06.008

Gastaldo, R.A., Adendorff, R., Bamford, M., Labandeira, C.C., Neveling, J., and Sims, H., 2005, Taphonomic trends of macrofloral assemblages across the Permian-Triassic boundary, Karoo Basin, South Africa: Palaios, no. 20, p. 479–497. 10.2110/palo.2004.P04-62

Groenewald, G.H., and Kitching, J.W., 1995, Biostratigraphy of the *Lystrosaurus* assemblage zone, *in* Rubidge, B.S., ed., Reptilian biostratigraphy of the Permian-Triassic Beaufort Group (Karoo Supergroup) South African Commission on Stratigraphy, Biostratigraphic Series 1: South Africa Commission on Stratigraphy, p. 29–34.

Hodgson, D.M., Di Celma, C., Brunt, R.L., and Flint, S.S., 2011, Submarine slope degradation and aggradation and the stratigraphic evolution of Channel-Levee systems: Journal of the Geological Society, no. 168, p. 625–628. doi:10.1144/0016-76492010-177

Holt, P.J., Allen, M.B., and Van Hunen, J., 2015, Basin formation by thermal subsidence of accretionary orogens: Tectonophysics, no. 639, p. 132–143. doi:10.1016/j.tecto.2014.11.021

Hoskin, P.W.O., and Black, L.P., 2000, Metamorphic zircon formation by solid-state recrystallization of protolith igneous zircon: Journal of Metamorphic Geology, no. 18, p. 423–439. doi:10.1046/j.1525-1314.2000.00266.x

Jones, G.E.D., Hodgson, D.M., and Flint, S.S., 2013, Contrast in the process response of stacked clinothems to the shelf-slope rollover: Geosphere, no. 9, p. 299–316. doi:10.1130/GES00796.1

Kleiman, L.E., and Japas, M.S., 2009, The Choiyoi volcanic province at 34°S-36°S (San Rafael, Mendoza, Argentina): Implications for the Late Palaeozoic evolution of the southwestern margin of Gondwana: Tectonophysics, no. 473, p. 283–299. doi:10.1016/j.tecto.2009.02.046

Kryza, R., Crowley, Q.G., Larionov, A., Pin, C., Oberc-Dziedzic, T., and Mochnacka, K., 2012, Chemical abrasion applied to SHRIMP zircon geochronology: An example from the

Variscan Karkonosze granite (Sudetes, SW Poland): Gondwana Research, no. 21, p. 757–767. doi:10.1016/j.gr.2011.07.007

Lanci, L., Tohver, E., Wilson, A., and Flint, S., 2013, Upper Permian magnetic stratigraphy of the lower Beaufort Group, Karoo Basin: Earth and Planetary Science Letters, no. 375, p. 123–134. doi:10.1016/j.epsl.2013.05.017

Lawver, L.A., Gahagan, L.M., and Coffin, M.F., 1992, The development of paleoseaways around Antarctica: Antarctic Research Series, no. 56, p. 7–30. doi:10.1029/AR056p0007

López-Gamundí, O., 2006, Permian plate margin volcanism and tuffs in adjacent basins of west Gondwana: Age constraints and common characteristics: *Journal of South American Earth* Sciences, no. 22, p. 227–238. doi:10.1016/j.jsames.2006.09.012

López-Gamundí, O., Fildani, A., Weislogel, A., and Rossello, E., 2013, The age of the Tunas formation in the Sauce Grande basin-Ventana foldbelt (Argentina): Implications for the Permian evolution of the southwestern margin of Gondwana: Journal of South American Earth Sciences, no. 45, p. 250–258. doi:10.1016/j.jsames.2013.03.011

López-Gamundi, O.R., and Rossello, E.A., 1998, Basin fill evolution and paleotectonic patterns along the Samfrau geosyncline: The Sauce Grande basin–Ventana foldbelt (Argentina) and Karoo Basin–Cape foldbelt (South Africa) revisited: Geologische Rundschau, no. 86, p. 819–834. doi:10.1007/s005310050179

Ludwig, K., 2008, A geochronological toolkit for Microsoft Excel: Berkeley Geochronology Ctr. Special Publication, no. 4, p. 77

Ludwig, K., 2009, SQUID 2: A user's manual: Berkeley Geochronology Center Special Publication, rev. 12 April, 2009, 5, p. 110.

Miller, J.S., Matzel, J.E.P., Miller, C.F., Burgess, S.D., and Miller, R.B., 2007, Zircon growth and recycling during the assembly of large, composite arc plutons: Journal of Volcanology and Geothermal Research, no. 167, p. 282–299. doi:10.1016/j.jvolgeores.2007.04.019

Moecher, D.P., and Samson, S.D., 2006, Differential zircon fertility of source terranes and natural bias in the detrital zircon record: Implications for sedimentary provenance analysis: Earth and Planetary Science Letters, no. 247, p. 252–266. doi:10.1016/j.epsl.2006.04.035

Ottone, E.G., Monti, M., Marsicano, C.A., De La Fuente, M. S., Naipauer, M., Armstrong, R., and Mancuso, A.C., 2014, A new Late Triassic age for the Puesto Viejo Group (San Rafael depocenter, Argentina): SHRIMP U–Pb zircon dating and biostratigraphic correlations across southern Gondwana: Journal of South American Earth Sciences, no. 56, p. 186–199. doi:10.1016/j.jsames.2014.08.008

Pankhurst, R.J., Rapela, C.W., Lopez De Luchi, M.G., Rapalini, A.E., Fanning, C.M., and Galindo, C., 2014, The Gondwana connections of northern Patagonia: Journal of the Geological Society, no. 171, p. 313–328. doi:10.1144/jgs2013-081

Pereira, M.F., Castro, A., Chichorro, M., Fernández, C., Díaz-Alvarado, J., Martí, J., and Rodríguez, C., 2014, Chronological link between deep-seated processes in magma chambers and eruptions: Permo-Carboniferous magmatism in the core of Pangaea (Southern Pyrenees): Gondwana Research, no. 25, p. 290–308. doi:10.1016/j.gr.2013.03.009

Retallack, G.J., and Krull, E.S., 1999, Landscape ecological shift at the Permian-Triassic boundary in Antarctica: Australian Journal of Earth Sciences, no. 46, p. 785–812. doi:10.1046/j.1440-0952.1999.00745.x

Riley, T.R., Flowerdew, M.J., and Whitehouse, M.J., 2012, U-Pb ion-microprobe zircon geochronology from the basement inliers of eastern Graham Land, Antarctic Peninsula: Journal of the Geological Society, London, no. 169, p. 381–393. doi:10.1144/0016-76492011-142

Rocha-Campos, A.C., Basei, M., Nutman, A., Kleiman, L., Varela, R., Llambia, E., Canile, F., and Darosa, C.R., 2011, 30 million years of Permian volcanism recorded in the Choiyoi igneous province (W Argentina) and their source for younger ash fall deposits in the Paraná Basin: SHRIMP U–Pb zircon geochronology evidence: Gondwana Research, no. 19, p. 509–523. doi:10.1016/j.gr.2010.07.003

Rocha-Campos, A.C., Basei, M.A.S., Nutman, A.P., and Dos Santos, P.R., 2006, SHRIMP U-Pb zircon geochronological calibration of the Late Paleozoic supersequence, Paraná Basin, Brazil, V South American Symposium on Isotope Geology, Punta del Este: Short Papers, p. 298–301.

Rubidge, B.S., 2000, Sequence analysis of the Ecca-Beaufort contact in the southern Karoo of South Africa: South African Journal of Geology, no. 103, p. 81–96. doi:10.2113/103.1.81

Rubidge, B.S., Erwin, D.H., Ramezani, J., Bowring, S.A., and De Klerk, W.J., 2013, High-precision temporal calibration of late Permian vertebrate biostratigraphy: U-Pb zircon constraints from the Karoo Supergroup, South Africa: Geology, no. 41, p. 363–366. doi:10.1130/G33622.1

Saylor, J.E., Stockli, D.F., Horton, B.K., Nie, J., and Mora, A., 2012, Discriminating rapid exhumation from syndepositional volcanism using detrital zircon double dating: Implications for the tectonic history of the Eastern Cordillera, Colombia: Geological Society of America Bulletin, no. 124, p. 762–779. doi:10.1130/B30534.1

Schwartz, J.J., Johnson, K., Mueller, P., Valley, J., Strickland, A., and Wooden, J.L., 2014, Time scales and processes of cordilleran batholith construction and high-sr/y magmatic pulses: evidence from the Bald Mountain batholith, northeastern Oregon: Geosphere, v. 10, no. 6, p. 1456–1481.

Shen, S.-Z., and others, 2011, Calibrating the end-Permian mass extinction: Science, no. 334, p. 1367–1372. 10.1126/science.1213454

Sircombe, K.N., and Stern, R.A., 2002, An investigation of artificial biasing in detrital zircon U-Pb geochronology due to magnetic separation in sample preparation: Geochimica Et Cosmochimica Acta, no. 66, p. 2379–2397. doi:10.1016/S0016-7037(02)00839-6

Smith, R.M.H., 1995, Changing fluvial environments across the Permian-Triassic boundary in the Karoo Basin, South Africa, and possible causes of tetrapod extinctions: Palaeogeography, Palaeoclimatology, Palaeoecology, no. 117, p. 81–104. doi:10.1016/0031-0182(94)00119-S

Smith, R.M.H., and Ward, P.D., 2001, Pattern of vertebrate extinctions across an event bed at the Permian-Triassic boundary in the Karoo basin of South Africa: Geology, no. 29, p. 1147–1150. doi:10.1130/0091-7613(2001)029<1147:POVEAA>2.0.CO;2

Spalletti, L.A., Fanning, C.M., and Rapela, C.W., 2008, Dating the Triassic continental rift in the southern Andres: The Potrerillos formation, Cuyo basin, Argentina: Geologica Acta, no. 63, p. 267–283.

Surpless, K.D., Graham, S.A., Covault, J.A., and Wooden, J., 2006, Does the Great Valley Group contain Jurassic strata?

Reevaluation of the age and early evolution of a classic forearc basin: Geology, no. 34, p. 21–24. doi:10.1130/G21940.1.

Tankard, A., Welsink, H., Aukes, P., Newton, R., and Stettler, E., 2009, Tectonic evolution of the Cape and Karoo basins of South Africa: Marine and Petroleum Geology, no. 26, p. 1379–1412. doi:10.1016/j.marpetgeo.2009.01.022

Veevers, J.J., 2004, Gondwanaland from 650-500 Ma assembly through 320 Ma merger in Pangea to 185-100 Ma breakup: Supercontinental tectonics via stratigraphy and radiometric dating: Earth-Science Reviews, no. 68, p. 1–132. doi:10.1016/j.earscirev.2004.05.002

Veevers, J.J., Cole, D.I., and Cowan, E.J., 1994a, Southern Africa: Karoo basin and Cape fold belt, *in* Veevers, J.J., and Powell, C. M., eds. Permian-Triassic Pangean basins and Foldbelts along the Panthalassan margin of Gondwanaland: Boulder, Colorado, G.S.A. Memoir, v. 184, p. 223–279.

Veevers, J.J., Powell, C.M., Collinson, J.W., and López-Gamundí, O.R., 1994b, Synthesis, *in* Veevers, J.J., and Powell, C.M., eds., Permian-Triassic Pangean basins and Foldbelts along the Panthalassan margin of Gondwanaland: Boulder, Colorado, G.S.A. Memoir, v. 184, p. 223–279.

Vorster, C., 2013, Laser ablation ICP-MS age determination of detrital zircon populations in the Phanerozoic Cape and Lower Karoo Supergroup (South Africa) and correlatives in Argentina [Ph.D. thesis]: University of Johannesburg.

Weislogel, A., Brunt, R.L., Flint, S., Fildani, A., and Rothfuss, J., 2011, Constraints on deepwater sedimentation in the Karoo Basin, South Africa, from U-Pb Geochronology of ash interbeds: AAPG Search and Discovery, Article #90124.

Wild, R., Flint, S., and Hodgson, D., 2009, Stratigraphic evolution of the upper slope and shelf edge in the Karoo Basin, South Africa: Basin Research, no. 21, p. 502–527. doi:10.1111/j.1365-2117.2009.00409.x

Wilson, A., Flint, S., Payenberg, T., Tohver, E., and Lanci, L., 2014, Architectural styles and sedimentology of the fluvial lower Beaufort Group, Karoo Basin, South Africa: Journal of Sedimentary Research, no. 84, p. 326–348. doi:10.2110/jsr.2014.28

Zeigler, A.M., Scotese, C.R., and Barrett, S.F., 1983, Mesozoic and Cenozoic paleogeographic maps, *in* Brosche, P., and Sundermann, J., eds., Tidal friction and the earth's rotation II: New York, Springer-Verlag, p. 240–252.